

**New shell closure for neutron-rich Sn isotopes**

S. Sarkar\*

*Department of Physics, Bengal Engineering and Science University, Shibpur, Howrah 711103, India*

M. Saha Sarkar†

*Nuclear Physics Division, Saha Institute of Nuclear Physics, Kolkata 700064, India*

(Received 11 October 2009; revised manuscript received 11 June 2010; published 29 June 2010)

The variation of  $E(2_1^+)$  of  $^{134-140}\text{Sn}$  calculated with empirical SMPN interaction has striking similarity with that of experimental  $E(2_1^+)$  of even-even  $^{18-22}\text{O}$  and  $^{42-48}\text{Ca}$ , showing clearly that  $N = 84-88$  spectra exhibit the effect of gradually filling up the  $\nu(2f_{7/2})$  orbital, which finally culminates in a new shell closure at  $N = 90$ . Realistic two-body interaction CWG does not show this feature. Spin-tensor decomposition of SMPN and CWG interactions and variations of their components with valence neutron number reveals that the origin of the shell closure at  $^{140}\text{Sn}$  lies in the three-body effects. Calculations with CWG3M, which is obtained by including a simple three-body monopole term in the CWG interaction, predict decreasing  $E(2_1^+)$  for  $^{136,138}\text{Sn}$  and a shell closure at  $^{140}\text{Sn}$ .

DOI: [10.1103/PhysRevC.81.064328](https://doi.org/10.1103/PhysRevC.81.064328)

PACS number(s): 21.60.Cs, 21.30.Fe, 23.20.Lv, 27.60.+j

**I. INTRODUCTION**

The evolution of shell structure away from stability [1] has been a topic of intense theoretical [2,3] and experimental [4–6] studies since the past decade. Theoretical studies have identified different reasons for the phenomenon of shell evolution with neutron or proton excess. Among the various components of the nucleon-nucleon interaction, the spin-orbit, tensor part, and three-body effect play important roles in the shell evolutions [1]. Owing to tensor interactions, the nuclear mean field undergoes variations with neutron excess. This leads to monopole migration [2]. It is observed for both proton-rich and neutron-rich nuclei. While approaching the neutron drip line, the neutron density becomes very diffused [3], which can also lead to shell quenching. For exotic light nuclei the well-established magic numbers for the stable nuclei are found to be modified or new magic numbers have evolved. At least four doubly magic oxygen isotopes have been observed [6–8]. They are  $^{14}\text{O}$ ,  $^{16}\text{O}$ ,  $^{22}\text{O}$ , and  $^{24}\text{O}$ . Brown and Richter [8] have framed a generalized new rule for magic numbers, valid especially for lighter nuclei. For heavier nuclei, experimental production of neutron-rich isotopes is more difficult. There are severe limitations in acquiring spectroscopic information on them owing to their low production rates and lifetimes. However, the shell evolution for neutron-rich nuclei above the doubly magic  $^{132}\text{Sn}$  core has recently become a topic of great interest. The Sn isotopes in particular pose many interesting problems [5,9–15] in the study of evolution of nuclear structure with increasing neutron number. The near constancy of the first  $2^+$  energy of Sn isotopes for  $A = 102-130$  at  $\simeq 1.2$  MeV is a textbook example for seniority-conserved spectra [16]. However, the two-valence neutron isotope of Sn just above  $^{132}\text{Sn}$ , that is,  $^{134}\text{Sn}$ , shows a sudden depression in  $2_1^+$  energy to 726 keV. This depressed energy is not only interesting

from the point of view of nuclear structure [17], it should also have an important implication for the  $r$ -process scenario [15].

Large basis untruncated shell-model (SM) calculations have been done using both realistic CWG [9,10,12] and empirical SMPN [10,11] (1+2)-body Hamiltonians. The two theoretical results differ dramatically for  $^{136,138}\text{Sn}$  [10]. The realistic interaction CWG predicts nearly constant energies of  $2_1^+$  states for the even-even Sn isotopes above the doubly magic  $^{132}\text{Sn}$  core, normally expected for singly magic nuclei. However, the empirical interaction SMPN predicts decreasing  $E(2_1^+)$  energies with increasing neutron number. The calculated energies with SMPN fit in the systematics [10] for the experimental  $E(2_1^+)$  energies of their isotones with  $Z > 50$ . They also agree with the trend shown by the Casten-Sherrill systematics for  $E(2_1^+)$  energy differences of Sn and Te isotopes having the same neutron number [10,15,17]. It has been shown in Ref. [10] that this nonconstancy of  $E(2_1^+)$  in Sn isotopes above  $^{132}\text{Sn}$  is a strong possibility. The prediction for dramatic decrease of the  $E(2_1^+)$  of neutron-rich Sn with increasing neutron number for  $N = 84-88$  using SMPN interaction was considered [10] to be an effect showing weakening of the  $Z = 50$  shell gap. However, the new result, which we report in this article, on  $^{140}\text{Sn}$ , its high  $2_1^+$  energy and its comparison with examples from other neutron-rich domains, clearly show that  $N = 84-88$  spectra with SMPN manifest the effect of gradually filling up the  $\nu(2f_{7/2})$  orbital, which finally culminates in a new shell closure at  $N = 90$ . We show that the realistic CWG predicts similar results; that is, decreasing  $2_1^+$  energies and a shell closure at  $^{140}\text{Sn}$  if three-body effects are included in it.

**II. SHELL-MODEL CALCULATIONS**

The CD-Bonn-potential-based realistic CWG [12] and the empirical SMPN [10,11] interactions have been used in the shell-model calculations in the valence space consisting

\*ss@physics.becs.ac.in

†maitrayee.sahasarkar@saha.ac.in

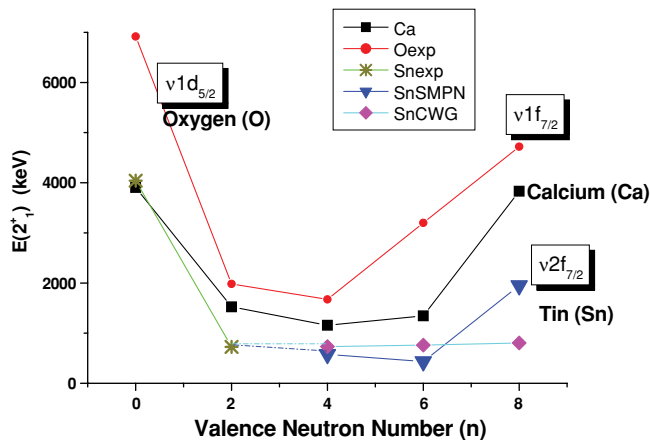


FIG. 1. (Color online) Comparison of  $E(2_1^+)$  energies as function of valence neutron number for oxygen (O), calcium (Ca), and Sn isotopes.

of  $\pi(1g_{7/2}, 2d_{5/2}, 2d_{3/2}, 3s_{1/2}, 1h_{11/2})$  and  $\nu(1h_{9/2}, 2f_{7/2}, 2f_{5/2}, 3p_{3/2}, 3p_{1/2}, 1i_{13/2})$  orbitals above the  $^{132}\text{Sn}$  core. The Hamiltonians have the same set of single-particle energies [10] of the valence orbitals but different sets of two-body interaction matrix elements (TBMEs). It should be noted that the neutron-neutron part of the CWG TBMEs is the same as that used by Kartamyshev *et al.* [9]. The shell-model codes OXBASH and NUSHELL@MSU have been used [18].

### III. RESULTS AND DISCUSSIONS

#### A. The new shell closure at $N = 90$ and comparison with other neutron-rich domains

The results for the  $E(2_1^+)$  energies of isotopes of Sn for  $A = 134\text{--}140$  have been shown in Fig. 1 as a function of valence neutrons above the  $^{132}\text{Sn}$  core. The experimental energies for  $^{132,134}\text{Sn}$  are shown in the figure. The predicted energies using CWG and SMPN interactions are compared. With CWG interaction, as mentioned earlier, the  $0_1^+ - 2_1^+$  spacing remains nearly constant at around 750 keV for  $^{136\text{--}142}\text{Sn}$ , except for a small increase at  $^{140}\text{Sn}$  [9] owing to the filling of the  $\nu(2f_{7/2})$  single-particle orbit. It has been identified [9] to be a weak shell closure at  $^{140}\text{Sn}$ . The seniority-conserved character of the low-lying spectra [16] observed for Sn isotopes below  $^{132}\text{Sn}$  is also preserved for isotopes above  $N = 82$  shell closure. The nearly constant  $E(2_1^+)$  value at around 1.2 MeV for  $52 \leq N \leq 80$  reduces to around 750 keV above  $N = 82$ . The same figure also contains variations of the experimental  $E(2_1^+)$  energies of even  $_{20}\text{Ca}$  isotopes from  $A = 40\text{--}48$  as a function of valence neutrons above the  $^{40}\text{Ca}$  core. Similarly, the variation of the experimental  $E(2_1^+)$  energies of even  $_8\text{O}$  isotopes from  $A = 16\text{--}24$  as a function of valence neutron numbers above  $^{16}\text{O}$  core are also shown. The variations of experimental  $E(2_1^+)$  with the valence neutron number for two different mass regions and shells show striking similarity with the theoretical predictions with SMPN in the  $^{132}\text{Sn}$  region. The gradual filling of the  $\nu(2f_{7/2})$  orbital by neutrons is very distinctively shown by the variation of  $E(2_1^+)$  from  $^{134\text{--}140}\text{Sn}$ . The  $E(2_1^+)$  for  $^{140}\text{Sn}$  is 1949 keV, showing a sudden

increase for  $N = 90$ , indicating a closed-shell structure for  $^{140}\text{Sn}$ .

The trend is very similar to that observed for neutron-rich isotopes of Ca while filling up the  $\nu(1f_{7/2})$  orbital and that shown by neutron-rich oxygen isotopes while filling up the  $\nu(1d_{5/2})$  single-particle orbital (Fig. 1). In the  $sd$  shell a gap of  $\simeq 850$  keV is observed between the  $\nu(1d_{5/2})$  and the  $\nu(2s_{1/2})$  single-particle orbitals. The experimental energies of the  $2_1^+$  states for the  $N = 10$  and 12 isotones are similar for elements with  $Z = 6, 8, 10$ , and 12 [6,7]. At  $N = 14$ , where the  $1d_{5/2}$  gets completely filled up, the  $2_1^+$  energies of the  $Z = 6, 10$ , and 12 remain nearly the same. However, the shell closure at  $N = 14$  for  $^{22}\text{O}$  with 6 neutrons in  $\nu(1d_{5/2})$  is indicated by the fact that  $2_1^+$  state energy ( $= 3.199$  MeV) in it is almost twice of that in the adjacent  $N = 10$  and 12 isotopes of oxygen. With the filling up of the  $\nu(2s_{1/2})$  orbital, the increase in  $2_1^+$  energy [ $E(2_1^+) = 4.72$  MeV] in  $^{24}\text{O}$  is much more dramatic, indicating another new shell gap at  $N = 16$  for  $Z = 8$  that is not present for  $Z = 6, 10$ , and 12. It has been discussed [6] that the mechanism behind the appearance of these new shell gaps for the oxygen isotopes is the tensor force. With protons present in the  $\pi(1d_{5/2})$  orbital in Ne and Mg isotopes, the  $\nu(1d_{3/2})$  orbital is drawn down in energy via the isospin component of the tensor force, thereby reducing the  $N = 16$  shell gap. A similar situation also prevails around  $^{140}\text{Sn}$ .

#### B. The effective single-particle energies

To put forward further evidence and to understand the shell closure at  $^{140}\text{Sn}$  more precisely, the effective single-particle energies (ESPEs) [2] for the neutron orbitals for the two Hamiltonians have been compared. The ESPE is defined as the bare single-particle energy (SPE) added with the monopole part of the diagonal TBMEs. The bare SPE is originated from the interaction of a valence nucleon with the doubly closed core. The monopole interaction contribution is the  $(2J + 1)$  weighted average of the diagonal TBME, which arises from the interaction of a valence nucleon with the other valence nucleons.

##### 1. Shell closure at $N = 90$ for Sn isotopes

The ESPE for the configurations  $\nu(2f_{7/2})^n$  in  $^{132\text{--}140}\text{Sn}$  with valence neutron number  $n$  varying from 0 to 8 are shown in Fig. 2. For both SMPN and CWG, the energy gap between  $\nu(2f_{7/2})$  and  $\nu(3p_{3/2})$  single-particle orbitals is 854 keV for the  $^{132}\text{Sn}$  core. However, the gap between the corresponding ESPEs increases to 2.246 MeV at  $N = 90$  with SMPN. This gap is sufficient to make  $^{140}\text{Sn}$  a doubly magic nucleus. For CWG this gap does not show any increase but instead decreases slightly to 826 keV.

##### 2. Onset of collectivity at $N = 90$ for $Z \geq 54$

It has been observed experimentally that  $N = 90$  is suitable for onset of deformation for nuclei above Sn (like Xe, Ba, etc.) [7]. Casten *et al.* have discussed [19] that with the increase in the number of protons in the  $\pi(1h_{11/2})$  orbital, its energy decreases if its spin orbit partner  $\nu(1h_{9/2})$  orbit is occupied.

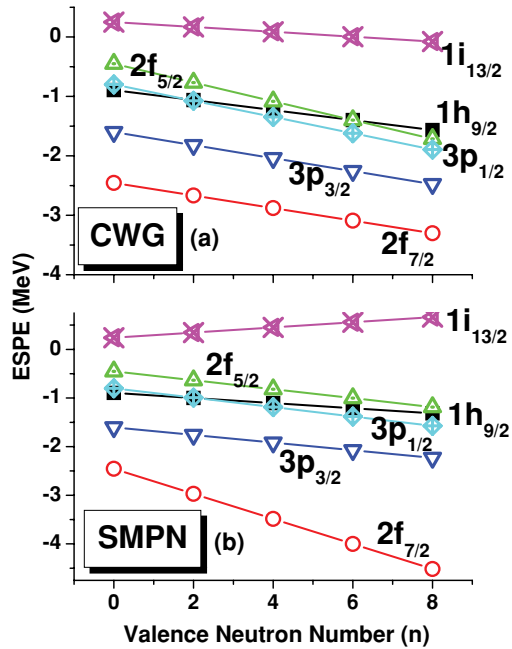


FIG. 2. (Color online) The ESPEs of the neutron single-particle orbitals for (a) CWG and (b) SMPN with increasing valence neutron number for  $Z = 50$ .

Therefore, the energy of the deformed configuration also comes down. By  $N = 90$ , the deformed configuration crosses the spherical one, realizing the shape transition point [19]. However, for the  $N = 90$  isotope of Sn nucleus, a distinct shell closure is predicted by the SMPN results, while CWG denotes it to be a weak one. The presence of valence protons above the inert core is essential [19,20] for onset of collectivity. So the ESPEs for SMPN which indicate the features of a shell closure for  $Z = 50$  at  $N = 90$ , should also indicate the possibility of onset of deformation at  $N = 90$  with increasing  $Z$ . The spacings between the ESPEs of neutron orbitals at  $N = 90$  for  $Z$  increasing from 50 to 58 do not show much variation. However, if the ESPEs for proton orbitals for  $N = 90$  with  $\nu(2f_{7/2})^8$  are plotted (Fig. 3), substantial reduction of the  $\pi(1g_{7/2})$  and  $\pi(2d_{5/2})$  energy gap is observed with increasing  $Z$ , which may favor onset of collectivity for  $Z \geq 54$ . Thus,

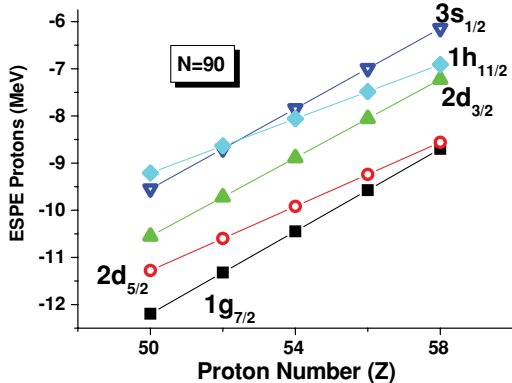


FIG. 3. (Color online) The ESPEs of the proton single-particle orbitals for SMPN with increasing proton number for  $N = 90$ .

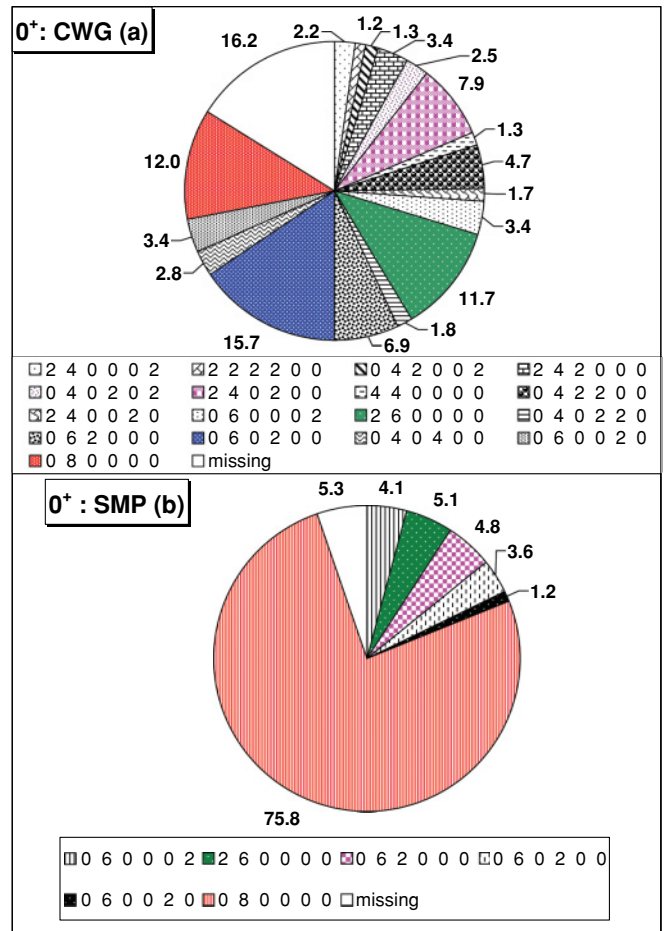


FIG. 4. (Color online) The decomposition of the wave functions for  $0^+$  states obtained using (a) CWG and (b) SMPN. The partitions indicate the occupancy of the single-particle orbitals in the following sequence,  $\nu(1h_{9/2}, 2f_{7/2}, 2f_{5/2}, 3p_{3/2}, 3p_{1/2}, 1i_{13/2})$ . See text for details.

SMPN, along with predicting a new shell closure at  $N = 90$  for Sn isotopes, also reproduces onset of collectivity at this neutron number for higher  $Z$ .

### C. The wave functions

To identify the structural difference between the two predictions, the wave functions have been compared. The composition of the wave functions for  $0^+$  ground states obtained with CWG and SMPN are shown in Figs. 4(a) and 4(b), respectively. For CWG results, the  $0^+$  ground state has a highly fragmented structure. Twelve percent of the state originates from the  $\nu(2f_{7/2})^8$  partition, 15.7% from the  $\nu(2f_{7/2})^6(3p_{3/2})^2$  partition, and 11.7% from the  $\nu(1h_{9/2})^2(2f_{7/2})^6$  partition. The missing component shown in the wave-function composition represents contribution from the partitions, each of which contributes less than 1%. The missing component here is 16.2%. The average occupancy for the  $\nu(2f_{7/2})$  orbital in the  $0^+$  state is 5.131; that for  $\nu(3p_{3/2})$  is 1.005. For the  $2^+$  state maximum, 10.1% is contributed by a single partition, viz.  $\nu(2f_{7/2})^6(3p_{3/2})^2$ . The missing component increases to

30.3%, indicating large configuration mixing. The occupancies of  $\nu(2f_{7/2})$  and  $(3p_{3/2})$  are 4.731 and 1.359, respectively. So the nature of the interaction favors large configuration mixing conserving seniority as far as possible.

In contrast to CWG results, with SMPN the  $0^+$  ground state originates primarily (75.8%) from the  $\nu(2f_{7/2})^8$  partition. The  $\nu(2f_{7/2})$  is also nearly full, viz., its occupancy is 7.439. However, for the  $2_1^+$  state, 69.1% originates from the  $\nu(2f_{7/2})^7(3p_{3/2})^1$ . The occupancies of  $\nu(2f_{7/2})$  and  $(3p_{3/2})$  are 6.4 and 1.08, respectively. For  $0_1^+$  and  $2_1^+$ , the missing components are 5.3% and 9.8%, respectively. So SMPN favors the purer structure of the low-lying states and shows characteristics of  $\nu(2f_{7/2})$  multiplets.

### D. The spin-tensor decomposition

To analyze the origin of this new shell closure, the important physical aspects of both the residual interactions are extracted by a spin-tensor decomposition [21] of the TBMEs. The nomenclature for the separated interaction components has been adopted from Ref. [22]. They are central, antisymmetric spin-orbit (ALS), spin-orbit (LS), and tensor. Figure 5 shows this decomposition. For SMPN, the central and ALS part for  $2f_{7/2}$ - $2f_{7/2}$  TBMEs account for a majority of the downward shift of the ESPE of  $2f_{7/2}$  with increasing valence neutron number ( $n$ ). The TBMEs involving  $3p_{3/2}$  are not modified in SMPN. They have dominant contribution from the central part. The central parts of  $2f_{7/2}$  and  $3p_{3/2}$  vary with similar slopes for increase in  $n$ . So the variation in ALS part is primarily responsible for this observed shell gap at  $N = 90$ .

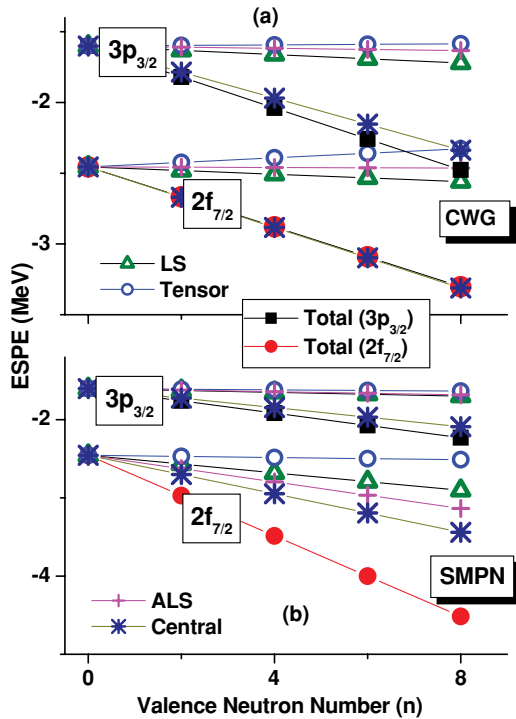


FIG. 5. (Color online) The spin-tensor decomposition of neutron ESPEs for (a) CWG and (b) SMPN with increasing valence neutron number.

Even though the neutron-neutron TBMEs involving  $3p_{3/2}$  orbital cannot be adjusted at present owing to lack of data, it can be safely assumed that the ESPE of this orbital will not have a steeper down-sloping trend than that of  $2f_{7/2}$  closing the presently observed  $2f_{7/2}$ - $3p_{3/2}$  gap at  $N = 90$ . It has been found for Ca isotopes that the monopole contribution of  $f_{7/2}$ - $p_{3/2}$  is positive, in contrast to the negative values of  $f_{7/2}$ - $f_{7/2}$  terms [1].

The ALS component in the TBMEs corresponds to those LS-coupled matrix elements which have  $S \neq S'$ , that is, terms nondiagonal in  $S$  (spin). Thus, these terms do not conserve total spin of the matrix elements [23,24]. However, the interactions which are parity conserving and isospin conserving must also conserve the total spin. Bare nucleon-nucleon force contains no ALS term [21,23,24]. However, effective interaction is not simply related to bare nucleon-nucleon force. Core polarization corrections to the  $G$  matrix give rise to nonzero but small ALS matrix elements. A characteristic feature common to many empirical effective interactions is strong ALS components in the TBMEs [23]. It usually arises from inadequate constraint by the data. It indicates the important contributions from higher-order renormalization or many body forces to the effective interactions. In empirical SMPN, such many-body effects might have been included in some way through the modification of important TBMEs. Thus, it is natural [1] to conjecture that realistic CWG differs from SMPN owing to the absence of any information of three-body effect in the CWG TBMEs.

### E. The three-body effects

At this point it is important to note that SM calculations using two-body realistic interactions derived from the free nucleon-nucleon force fail to reproduce some shell closures [1]. It is now rather well established that increase of the  $1d_{5/2}$ - $2s_{1/2}$  gap for  $Z = 8$  and  $1f_{7/2}$ - $2p_{3/2}$  gap for  $Z = 20$  (as a function of neutron number), required to explain empirical data, are not obtained in the calculations with these interactions. It has been shown that the three-body forces have to be taken into account to reproduce these shell gaps [1,25–27]. Thus, many of the previously observed discrepancies are now solved. Otsuka *et al.* [27] have proposed a three-body  $\Delta$ -hole mechanism to explain these shell gaps and they have shown that three-body forces are necessary to explain why the doubly magic  $^{24}\text{O}$  nucleus is the heaviest oxygen isotope. Zuker [26] showed earlier that a very simple three-body monopole term can solve practically all the spectroscopic problems in the  $p$ ,  $sd$ , and  $fp$  shells those were earlier assumed to need drastic revisions of the realistic two-body potentials.

As a next step, therefore, in this attempt of analyzing the new shell gap, we have incorporated a simple three-body monopole term in CWG as prescribed in Refs. [25,26]. We have incorporated corrections in  $2f_{7/2}$ - $2f_{7/2}$  and  $2f_{7/2}$ - $3p_{3/2}$  TBMEs similar to those in KB3 for  $1f_{7/2}$ - $1f_{7/2}$  and  $1f_{7/2}$ - $2p_{3/2}$  TBMEs. However, as the mass regions considered in KB3 ( $A > 40$ ) and the present case ( $A > 132$ ) are quite far off, we have included the effect of mass scaling. The scaling is given by  $(40/132)^{(1/3)}$  factor. This factor reduces the effect of three-body correction on CWG compared to that

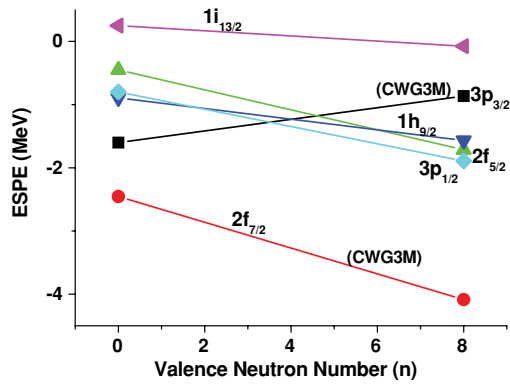


FIG. 6. (Color online) The neutron ESPEs for CWG3M with increasing valence neutron number. See text for details.

in KB3. The correction terms included in the TBMEs are  $V_{ffff}^{J,T=1}(\text{CWG3M}) = V_{ffff}^{J,T=1}(\text{CWG}) - 74$  keV for  $J = 0, 4$  and 6 and  $V_{ffff}^{J=2,T=1}(\text{CWG3M}) = V_{ffff}^{J=2,T=1}(\text{CWG}) - 208$  keV and  $V_{frfr}^{J,T=1}(\text{CWG3M}) = V_{frfr}^{J,T=1}(\text{CWG}) + 201$  keV for  $J = 2, 3, 4,$  and 5. Here  $f$  stands for  $2f_{7/2}$  and  $r$  stands for  $3p_{3/2}$ . It should be noted that the correction factor will be effective for nuclei for which the valence neutron number  $n \geq 3$ . The ESPEs after this correction are plotted in Fig. 6. A shell gap for  $N = 90$  now appears with CWG3M, which is very close to that with SMPN. The  $E(2_1^+)$  energies of  $^{136,138}\text{Sn}$  are 0.639 and 0.633 MeV, respectively. The  $E(2_1^+)$  energy of  $^{140}\text{Sn}$  predicted by CWG3M (1.889 MeV) is close to that predicted by SMPN (1.949 MeV). Comparison of the wave functions (Sec. III C) of the  $0_{g.s.}^+$  and  $2_1^+$  states with CWG and SMPN showed that whereas CWG favors large configuration mixing conserving seniority as far as possible, the SMPN favors the purer structure of the low-lying states, characteristics of  $\nu(2f_{7/2})^8$  and  $\nu(2f_{7/2})^7(3p_{3/2})$  multiplets. For CWG3M, the wave function composition for the  $0_{g.s.}^+$

is (70.4%) from the  $\nu(2f_{7/2})^8$  partition, similar to SMPN (75.8% Sec. III C). However, owing to overestimation of the up-sloping trend of  $\nu(3p_{3/2})$  ESPE (Fig. 6), for  $2_1^+$  state, 29.0% originates from the  $\nu(2f_{7/2})^6(1h_{9/2})^2$  and 9.6% from  $\nu(2f_{7/2})^6(2f_{5/2})^2$ . The effective energy gap between  $\nu(2f_{7/2})$  and  $\nu(2f_{5/2})$  (the lowest orbital that contributes to the composition of  $2_1^+$  state) single-particle orbitals is 2.370 MeV (Fig. 6).

#### IV. CONCLUSIONS

In conclusion, we find that comparison with the systematics of  $2_1^+$  energies of other  $n$ -rich domains and the spin-tensor decomposition of the two interactions establish the new shell closure at  $^{140}\text{Sn}$ . The ALS term incorporates in it the contributions of many-body forces in the empirical interaction. A large contribution of this term in the ESPE of  $2f_{7/2}$  in empirical interaction SMPN has been observed. It is found to be responsible for the gap observed in SMPN results. The CWG indicates a weak shell closure at  $^{140}\text{Sn}$ . A simple three-body monopole term has been included in CWG to get CWG3M. The new CWG3M predicts a shell gap at  $N = 90$  for Sn isotopes as well as decreasing  $2_1^+$  energies for  $^{136,138}\text{Sn}$ , similar to that from SMPN. This also indicates that the three-body effect plays an important role for shell evolution in neutron-rich Sn isotopes above  $^{132}\text{Sn}$ , as also observed in  $sd$  and  $fp$  shells. The anomalously depressed  $2_1^+$  states in Sn isotopes having  $N = 84-88$  and the new shell closure for  $N = 90$  might have interesting consequences for the  $r$ -process nucleosynthesis.

#### ACKNOWLEDGMENTS

The authors thank Waldek Urban for stimulating discussions on the issues in this mass region. Special thanks are owed to B. A. Brown for his help in providing us the OXBASH (Windows Version) and the NUSHELL@MSU CODES.

- [1] O. Sorlin and M. G. Porquet, *Prog. Part. Nucl. Phys.* **61**, 602 (2008).
- [2] T. Otsuka, T. Suzuki, R. Fujimoto, H. Grawe, and Y. Akaishi, *Phys. Rev. Lett.* **95**, 232502 (2005).
- [3] J. Dobaczewski, I. Hamamoto, W. Nazarewicz, and J. A. Sheikh, *Phys. Rev. Lett.* **72**, 981 (1994); J. Dobaczewski, N. Michel, W. Nazarewicz, M. Ploszajczak, and J. Rotureau, *Prog. Part. Nucl. Phys.* **59**, 432 (2007).
- [4] G. de Angelis, *Prog. Part. Nucl. Phys.* **59**, 409 (2007), and references therein.
- [5] J. P. Schiffer *et al.*, *Phys. Rev. Lett.* **92**, 162501 (2004).
- [6] M. Górska *et al.*, *Phys. Lett. B* **672**, 313 (2009); P. G. Thirolf *et al.*, *ibid.* **485**, 16 (2000); R. Kanungo *et al.*, *Phys. Rev. Lett.* **102**, 152501 (2009); C. R. Hoffman *et al.*, *Phys. Lett. B* **672**, 17 (2009).
- [7] [<http://www.nndc.bnl.gov>].
- [8] B. A. Brown and W. A. Richter, *Phys. Rev. C* **72**, 057301 (2005).
- [9] M. P. Kartamyshev, T. Engeland, M. Hjorth-Jensen, and E. Osnes, *Phys. Rev. C* **76**, 024313 (2007), and references therein.
- [10] S. Sarkar and M. S. Sarkar, *Phys. Rev. C* **78**, 024308 (2008).
- [11] S. Sarkar, M. S. Sarkar, *Eur. Phys. Jour. A* **21**, 61 (2004), and references therein; *Phys. Rev. C* **81**, 039803 (2010).
- [12] B. A. Brown, N. J. Stone, J. R. Stone, I. S. Towner, and M. Hjorth-Jensen, *Phys. Rev. C* **71**, 044317 (2005).
- [13] S. Sarkar and M. S. Sarkar, *Phys. Rev. C* **64**, 014312 (2001), and references therein.
- [14] L. Coraggio, A. Covello, A. Gargano, and N. Itaco, *Phys. Rev. C* **72**, 057302 (2005), and references therein.
- [15] S. Sarkar and M. Saha Sarkar, in *Proceedings of 4th International Workshop on Nuclear Fission and Fission Product Spectroscopy, France, 13-16 May 2009* (to be published).
- [16] R. F. Casten, *Nuclear Structure from a Simple Perspective* (Oxford University Press, Oxford, 1990), p. 120.
- [17] R. F. Casten and B. M. Sherrill, *Prog. Part. Nucl. Phys.* **45**, 171 (2000).
- [18] B. A. Brown *et al.*, OXBASH for Windows PC, MSU-NSCL Report No. 1289, 2004; B. A. Brown and W. D. M. Rae, NUSHELL@MSU, MSU-NSCL Report, 2007.

- [19] R. F. Casten, D. D. Warner, D. S. Brenner, and R. L. Gill, *Phys. Rev. Lett.* **47**, 1433 (1981).
- [20] R. Kshetri, M. S. Sarkar, and S. Sarkar, *Phys. Rev. C* **74**, 034314 (2006).
- [21] M. W. Kirson, *Phys. Lett. B* **47**, 110 (1973); K. Yoro, *Nucl. Phys. A* **333**, 67 (1980).
- [22] B. A. Brown, W. A. Richter, and B. H. Wildenthal, *J. Phys. G* **11**, 1191 (1985).
- [23] K. Yoshinada, *Phys. Rev. C* **26**, 1784 (1982).
- [24] B. A. Brown, W. A. Richter, and R. E. Julies, *Ann. Phys.* **182**, 191 (1988).
- [25] A. Poves and A. Zuker, *Phys. Rep.* **70**, 235 (1981).
- [26] A. P. Zuker, *Phys. Rev. Lett.* **90**, 042502 (2003).
- [27] T. Otsuka, T. Suzuki, J. D. Holt, A. Schwenk, and Y. Akaishi, [arXiv:0908.2607v2](https://arxiv.org/abs/0908.2607v2).